Computers and Electronics in Agriculture 140 (2017) 452–460

Contents lists available at ScienceDirect

Computers and Electronics in Agriculture

journal homepage: www.elsevier.com/locate/compag

Machine vision based soybean quality evaluation

Md Abdul Momin [a,b,d,*], Kazuya Yamamoto [b], Munenori Miyamoto [c], Naoshi Kondo [b], Tony Grift [d]

[a] Department of Farm Power and Machinery, Bangladesh Agricultural University, Mymensingh 2202, Bangladesh
[b] Graduate School of Agriculture, Kyoto University, Kitashirakawa-Oiwakecho, Sakyo-ku, Kyoto 606-8502, Japan
[c] Agricultural Research Center, Agricultural Operations Business, Yanmar Co., Ltd., 2481, Umegahara Maibara, Shiga 521-8511, Japan
[d] Department of Agricultural and Biological Engineering, University of Illinois at Urbana–Champaign, 1304 West Pennsylvania Avenue, Urbana, IL 61801, USA

ARTICLE INFO

Article history:
Received 26 August 2016
Received in revised form 9 May 2017
Accepted 22 June 2017

Keywords:
Foreign materials identification
Front lit
Backlit
Image processing

ABSTRACT

A novel proof of concept was developed targeted at the detection of Materials Other than Grain (MOGs) in soybean harvesting. Front lit and back lit images were acquired, and image processing algorithms were applied to detect various forms of MOG, also known as dockage fractions, such as split beans, contaminated beans, defect beans, and stem/pods. The HSI (hue, saturation and intensity) colour model was used to segment the image background and subsequently, dockage fractions were detected using median blurring, morphological operators, watershed transformation, and component labelling based on projected area and circularity. The algorithms successfully identified the dockage fractions with an accuracy of 96% for split beans, 75% for contaminated beans, and 98% for both defect beans and stem/pods.

1. Introduction

Soybean (*Glycine max*) is the world's most important legume crop. The harvesting of soybean typically employs a grain head that transports the plants' pods into a threshing/separation/cleaning mechanism. Various types of combine harvester have been used for soybean since the mid-1920s but little progress has been made in improving grain quality until about 1970 (Sumner, 2000).

The amount of foreign material mixed in with the grain in the tank (frequently referred to as Material Other than Grain or MOG) is an important quality parameter, because after harvesting, the product must be sorted and graded based on various physical quality attributes (Chetna, 2013). In addition, the presence of MOG affects the processing equipment, efficiency of the oil extraction process and the quality of the final products (Islas-Rubio and Higuera-Ciapara, 2002). Moreover, the authors recommended that soybeans containing certain MOG levels should be cleaned to facilitate the production of high quality end products.

The level of contamination with MOG is highly dependent upon the combine settings. Typically, improper adjustments, or the inability to make rapid adjustments, lead to the presence of foreign materials which ultimately affects the quality of the grain in the tank. The dominant combine setting affecting mechanical soybean damage is the threshing cylinder speed: over threshing causes beans that have surface cracks (here termed "cracked beans") or are broken in two or more parts (termed "split beans"), whereas under threshing fails to separate the beans from the pod. The cleaning sieves' opening setting, their oscillation frequency, and fan speed also affect the amount of MOG in the tank. Finally, improper setting of the combine header may cause the presence of soil and/or weed particles or other vegetative matter attached to the beans.

Typically, operators will use recommended settings for a specific combine, but without visual feedback from the grain quality in the tank, this can lead to grain damage and increased grain loss (Matsui, 1999; Takahara and Hayashi, 1996). A real-time grain quality indication could be used to efficiently adjust machine settings to reduce the amount of MOG as well as the level of damage to the grain itself (Craessaerts et al., 2007, 2008; Wallays et al., 2009). In this research, we developed a proof of concept of such an on-board grain quality monitoring system.

The development of sensing, localization, communication and computing technologies has enabled Precision Agriculture, where each step in production processes is monitored with the aim of improving product quality, keeping records and overall management. The method takes advantage of recent advances in sensing and digital image processing techniques, which have been successfully applied in quality control in the food and agricultural sectors (Abdullah et al., 2005; Brosnan and Sun, 2004; Chen et al., 2002; Rohit et al., 2011). For instance, mould contamination in soybean was detected with 80% accuracy using a simplified computer vision system (Gunasekaran et al., 1988). In addition, a lab scale grain

* Corresponding author at: Department of Farm Power and Machinery, Bangladesh Agricultural University, Mymensingh 2202, Bangladesh.
E-mail address: mominfpm@bau.edu.bd (M.A. Momin).

http://dx.doi.org/10.1016/j.compag.2017.06.023
0168-1699/

cleaning system using machine-vision-computed morphological features was designed, fabricated, and evaluated (Paliwal et al., 2004). Furthermore, a multispectral vision sensor for on-line measurement of weight percentage of MOG in the sample was proposed to efficiently adjust the combine settings (Wallays et al., 2009). Finally, in a recent study, a machine vision system was used to classify soybean frogeye, mildewed soybean, worm-infested soybean and damaged soybean with identification accuracies of 96%, 95%, 92%, and 92%, respectively (Tan et al., 2014).

The objective of this research was to develop a machine-vision based proof of concept of a grain quality monitoring system, targeted at application on a combine harvester.

2. Materials and methods

The machine vision subsystem of the grain quality monitoring concept comprised a digital camera, in combination with back, front and structured lighting. It used a container in which soybean samples were presented with common MOGs such as broken seeds, defect seeds, as well as leaf and pod material. Because of its overall popularity, a Fukuyutaka soybean variety was used, which was harvested in December 2011 in the Mie prefecture, Japan. Soybean samples were obtained directly from a combine harvester tank, at a moisture content of approximately 11%. The samples were kept in closed plastic bags and stored in a refrigerated chamber at approximately 12 °C. From the collected samples, 500 g material samples were chosen at random. Fig. 1(a) shows the most common anomalies in soybean samples, being (b) split beans, (c) stem/leaf material, (d) beans contaminated with soil particles, (e) beans infected by *Phomopsis longicolla*, a fungus that causes fine cracks in the seeds in which mould grows, (f) heat damaged beans and (g) beans with purple stains caused by the *Cercospora* fungus. The following classification terminology was used in this research:

(1) "normal": soybean seeds without damage
(2) "split": broken and cracked soybean seeds
(3) "contaminated": soybean seeds contaminated by soil or other vegetative contact
(4) "defect": soybean seeds affected by insects, mould and heat
(5) "stem/pods": pieces of the soybean pods or other plant parts

2.1. Image acquisition

To accommodate technical and financial constraints of the proposed grain quality monitoring system, a compact, rugged, low-cost, camera was chosen. Fig. 2(a) shows the 2MP portable WEB camera model: C905m, class: UXGA (Logicool Co., Ltd., JP). Besides a high quality camera, proper lighting is key to achieve optimal image quality (Chen et al., 2002; Gunasekaran, 1996). Most machine vision arrangements employ either front lighting, back lighting or structured lighting. Front lighting allows for the detection of surface features or textures whereas backlighting gives contrast information (Novini, 1990). In this project, cracked beans and stem/pods were detected through morphological features, requiring back lighting, whereas contaminated beans represent surface properties requiring front lighting. Therefore, both front and back lighting were employed alternatingly. To reduce the effect of halation (bright or purple coloured pixels) created on target objects, a ring type light unit (CCS Co., Ltd., Tokyo, Japan) with a polarization (PL) filter was chosen as shown in Fig. 2(b). The ring type light allowed placing the web camera inside the ring, adding to the system's compactness. For back lighting, a square type flat dome light unit (CCS Co., Ltd., Tokyo, Japan) was used as shown in Fig. 2(c). The flat dome light has a patterned face, which provides highly diffused light, allowing shadow free imaging. A power unit (CCS Co., Ltd., model: PD2-3024-2, Tokyo, Japan) was used to control the brightness of both lighting devices.

The image acquisition cell comprised the web camera, which was placed inside the ring LED unit, and fitted with a polarization filter. It was opposed by a glass object plate, which had a smooth and a rough side, backed up by the flat white LED unit (Fig. 3). The soybean samples were placed on the smooth side of the glass plate. The rough side of the glass plate faced the backlighting side, where the flat dome LED light acted as an additional diffusing panel. The distance between the ring LED and the object plate was maintained at 47 mm providing a field of view size of 50 mm × 50 mm. The described image acquisition system was patented in Japan (Patent No. 5780642) (Miyamoto et al., 2015).

Logicool Webcam Software V-1.1 (Logitech. Com., Romanel-sur-Morges, Switzerland) was used to set the camera's operating parameters and for image acquisition. After adjusting each parameter, the white balance was checked to avoid colour variations and shadow noise. Table 1 shows the final adjusted camera parameters used for imaging, whereas the white balance image of the background is shown in Fig. 4. The white balance images confirmed that the incident light was evenly distributed across the sampling area, yielding a high quality imaging scene.

Once the camera parameters were finalized, images were captured. Samples weighing approximately 10 g were imaged with a size of 1600 × 1200 pixels and a resolution of 24 pixel/mm. The sample image as shown in Fig. 5 contains ten "normal" beans, four "split" beans, four "contaminated" beans, four pieces of "defect" beans and one piece of "stem/pod", placed on the glass plate within the sampling area of 50 mm × 50 mm. The image resolution was

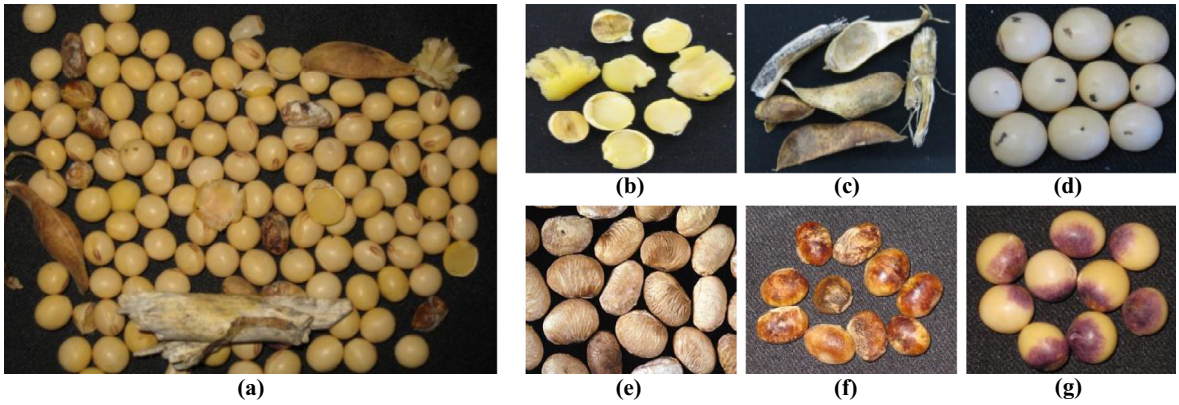

Fig. 1. Harvested soybean samples (a). Various dockage fractions found in the harvested samples: split beans (b), stem/pods (c), contaminated beans (d), and defected beans: in which Phomopsis causes fine cracks and mould (e), heat-damaged beans (f), purple stained beans caused by Cercospora Leaf Spot (g).

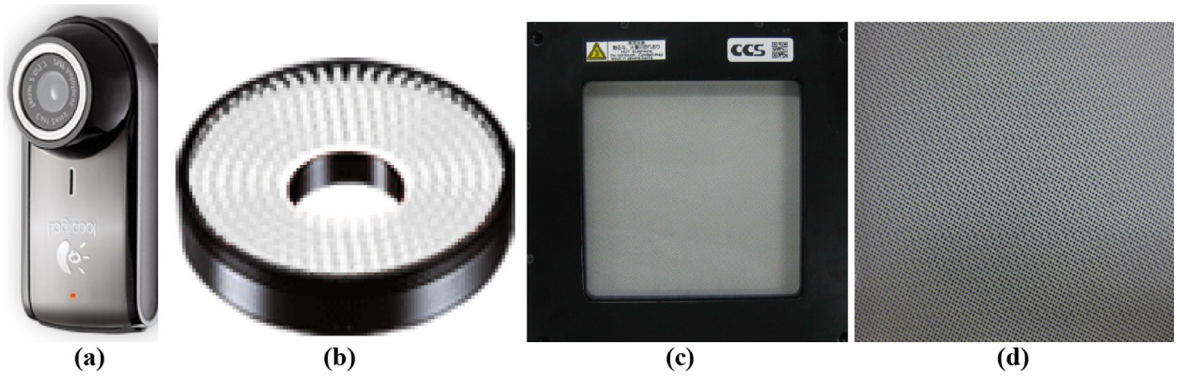

Fig. 2. Devices used for image acquisition: (a) web camera, (b) ring LED, (c) flat dome LED, and (d) dot pattern on flat light surface.

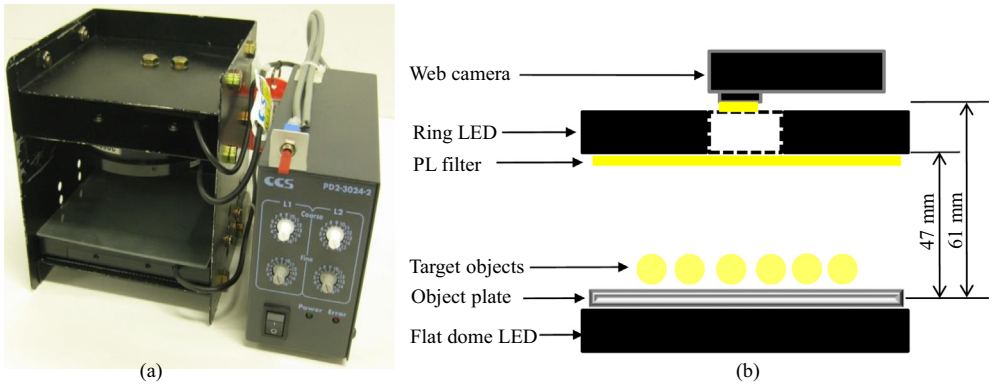

Fig. 3. Appearance (a) and schematic layout (b) of the utilized machine vision system.

Table 1
Camera calibration parameters.

Lighting panel	Shutter speed (sec)	Gain (db)	Brightness	Contrast	Colour intensity	Sharpness	White balance	Focus	Power control setting
Front	1/500	10000	4050	1255	1098	7490	10000	155	Max
Back	1/100	10000	4050	1255	1098	7490	10000	155	Max

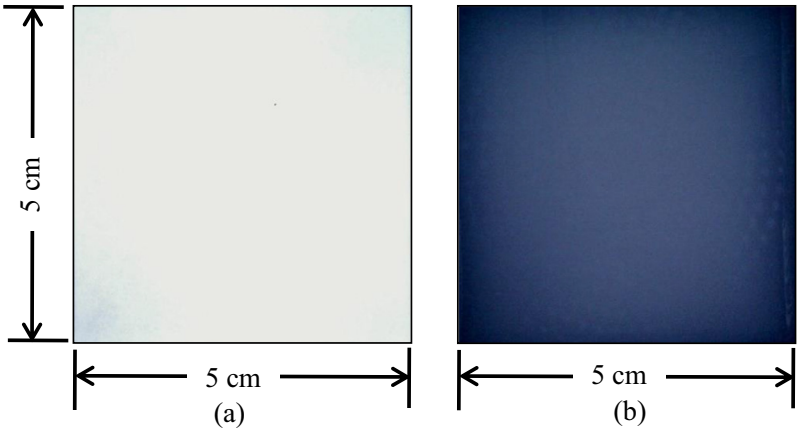

Fig. 4. White balance images of work piece: (a) white paper and (b) glass plate.

calculated by dividing the number of vertical pixels (1200) by the vertical field view of the image (50 mm). From Fig. 5 it is clear that front lit images allow for identification of normal beans (green circles), contaminated beans (pink circles), defect beans (yellow circles), and stem/pods (red circles). Back lit images allowed for the identification of split beans (blue circles). In total, 50 front and 50 back lit images were processed, accounting for approximately 500 g of material. A total of 620 normal soybeans, 70 split

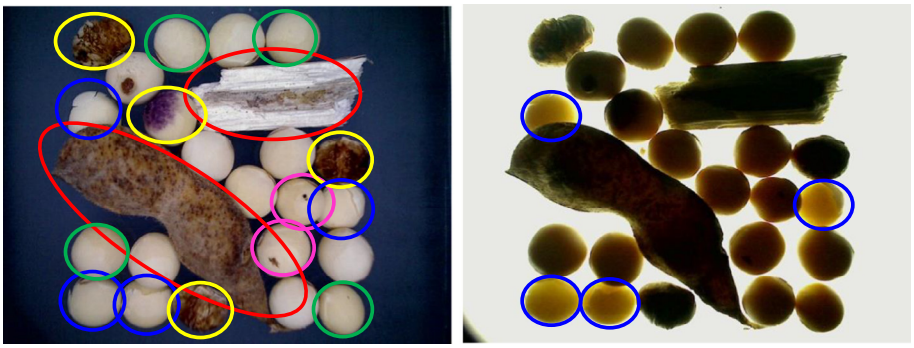

Fig. 5. Example of an acquired original colour image (left: front lit and right: back lit). (For interpretation of the references to colour in this figure legend, the reader is referred to the web version of this article.)

beans, 36 soil contaminated beans and 145 other objects (defect beans and stems/pods) were used for evaluation. The images were saved in the JPEG format.

2.2. Image pre-processing

The algorithms used in this study were written in Microsoft Visual C++, version 6.0. Post-processing of the resulting JPEG images was conducted using OpenCV (Open Source Computer Vision) library functions (Gary and Kaehler, 2008). To identify each target object, RGB (red, green, and blue) and HSI (hue, saturation and intensity) colour bands of the front and back lit images were used to threshold images and isolate the target objects from the image background. The HSI colour model represents the way the human eye senses colour more closely than colour models such as RGB or CMYK (cyan, magenta, yellow, key (black)) and is considered an ideal tool for developing image processing algorithms (Chun-Liang and Din-Chang, 2011; Gonzalez and Woods, 2002). The conversion from the RGB to the HSI colour space was accomplished using the following equations (Gonzalez and Woods, 2002).

$$H = \cos^{-1}\left\{\frac{0.5[(R-G)+(R-B)]}{[(R-G)^2+(R-B)(G-B)]^{1/2}}\right\} \quad (1)$$

$$S = 1 - \frac{3}{(R+G+B)}[\min(R,G,B)] \quad (2)$$

$$I = \frac{1}{3}(R+G+B) \quad (3)$$

Plotting HSI colour values of all the target objects and background created an image histogram. These served to determine the threshold value that allows for segmenting the source image, where pixels with colour values equal or greater than T are considered object related (presented in white pixels) and pixels with colour values lower than T are considered background related (presented in black pixels). After thresholding, various image processing techniques among which smoothing, opening, closing, debridging, as well as size and shape discrimination were performed. Median blur type smoothing and morphological opening and closing were used to remove single noise pixels (i.e. undesired pixels) in the segmented image. The watershed transform was applied to the processed images for de-bridging *i.e.* isolating overlapping and touching objects. The projected area of each identified object was determined by counting the number of pixels within the object boundary of a binary image and a *FloodFill* algorithm (Gary and Kaehler, 2008). This algorithm also creates a mask image, which was used to calculate the perimeter of the filled object (Laungrungthip, 2008). The circularity of each target object was calculated using Eq. (4) which uses the object's area and perimeter (Olson, 2011).

$$\text{Circularity} = \sqrt{\frac{4\pi \times \text{Area}}{\text{Perimeter}^2}} \quad (4)$$

3. Results and discussion

For clarity, the results are divided into the front lit images which were used to detect normal beans, contaminated beans, defect beans, as well as stem/pods, and back lit images which were used to detect split beans. Back lighting was used here because the external surface appearance of split beans is similar to normal beans, making it difficult to detect using a front lit image. The projected areas of normal beans, contamination locations on the beans, and split beans were calculated in pixels for further image processing operations and shown in Fig. 6. The projected area of normal soybeans ranged from 25,000 to 35,000 pixels, whereas the pixel size of soil contaminated points were ranged lower than 500 pixels. Five different sizes of split bean were found in the representative samples and classified as large, medium, small, threshed and over-threshed split.

3.1. Front lit image processing and segmentation

Fig. 7 shows the relationship between the HSI colour values of normal beans, defect beans, stem/pods, and the image background. Table 2 shows the range and mean of extracted HSI colour features of each object. The Saturation-Hue and Intensity-Hue histograms show distinct differences among the target objects and the background, making them useful for thresholding. The threshold limit was chosen from the minimum and maximum HSI values that were found among several points so as to separate normal soybeans from other objects. The minimum and maximum H, S and I threshold limits were 0–354, 0–15, and 126–211 respectively. Fig. 8 shows the procedure used for front lit image processing and detection of contaminated beans, defect beans and stem/pods.

3.1.1. Detection of contaminated beans

A contaminated bean is essentially a normal bean that features one or more connected contaminated areas on its surface. To detect normal soybeans, after image acquisition, the front lit images were converted into a binary form using selected threshold values (Table 2). However, there were noisy areas in the segmented imagery, which had colour values similar to the soybeans. To alleviate this problem, after image thresholding, median blur type smoothing, and one time opening using a morphological structured

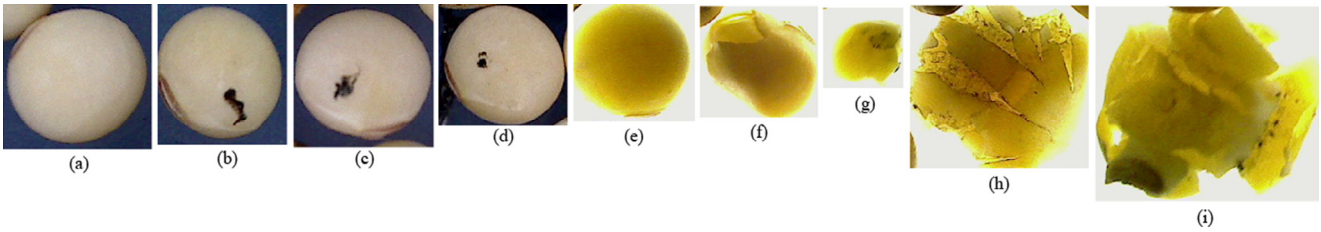

Fig. 6. Extracted projected area feature. (a) Regular soybean 25,000–35,000 pixels; various contaminated points: (b) 480 pixels, (c) 440 pixels, (d) 270 pixels; various split beans: (e) large split 25,000–35,000 pixels, (f) medium split 20,000 pixels, (g) small split 12,000 pixels, (h) threshed split <50,000 pixels, (i) over-threshed split >50,000 pixels.

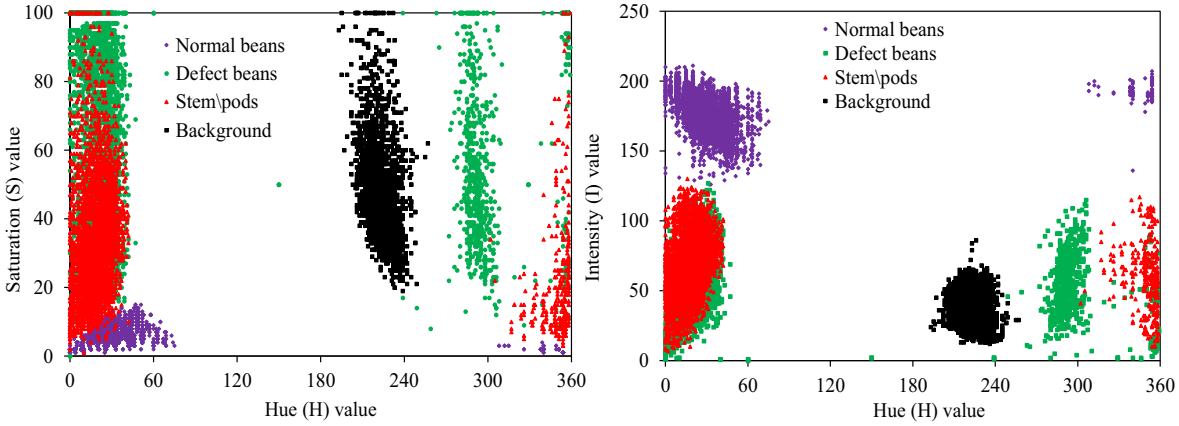

Fig. 7. Front lit image histograms of HSI components of target objects and image background.

Table 2
HSI colour features of front and back lit images.

Image type	Target objects	H			S			I		
		Max	Min	Mean	Max	Min	Mean	Max	Min	Mean
Front lit	Normal beans	354	0	36	15	0	6	211	126	176
	Defect beans	359	0	79	100	0	71	127	0	43
	Stem/pods	359	0	40	100	1	31	130	7	68
	Image background	257	193	223	100	19	45	86	12	43
Back lit	Split beans	64	29	44	100	29	90	183	46	97
	All other objects	358	0	38	100	1	83	238	1	28

element were applied. Subsequently, size and shape discrimination was performed by removing areas of a size and circularity lower than a certain threshold. The segmentation results of all normal and split soybeans are shown in Fig. 9(b). Subsequently, the segmented soybean image was inverted and filtered using the aforementioned area and circularity thresholds. The contaminated points (see Fig. 9(c)) were identified with 75% accuracy.

3.1.2. Detection of defect beans and stem/pods

From Fig. 7 and Table 2 it is clear that all target objects can be distinguished from the background as there are clear differences in HSI features. To segment normal beans, defect beans, and stem/pods, first a binary conversion was applied using threshold values H (193–257), S (19–100), and I (12–86), after which the image was inverted (Fig. 9(d)). To identify the boundary of each object, the watershed algorithm was applied (Fig. 9(e)), after which the inverted image (Fig. 9(d)) was subtracted from the boundary image (Fig. 9(e)) and the obtained de-bridging image (Fig. 9(f)). At this point, all target objects are isolated, which enabled identification of each object. Finally, to identify defect beans, as well as stem/pods, the de-bridged image (Fig. 9(f)) was subtracted from the normal/cracked bean image (Fig. 9(b)). After this, a size filtering operation was applied to remove any leftover noise pixels, yielding Fig. 9(h). The algorithm was able to detect defect beans and stem/pods with an accuracy of 98%.

3.2. Back lit image processing and segmentation

Back lighting produced a strong surface colour contrast between normal and split beans (Fig. 5), which enabled identification of the latter. Fig. 10 shows the Intensity-Hue and the Saturation-Hue values of the sample shown in right image of Fig. 5, which includes split beans, normal and defect beans, as well as stem/pods. The procedure used for the detection of split beans in back lit images is shown in Fig. 11.

A distinct difference in intensity (I) values between split beans and all other objects was observed (Fig. 10) and thus, to identify the split beans, thresholding was applied using the intensity attribute of the HSI colour model. However, some pixels of the normal beans' outer layer and stem/pods overlapped with the split bean pixels in the binary image. To eliminate these noisy regions, firstly a smoothing operation was applied followed by morphological opening (erosion followed by dilation) and closing (dilation followed by erosion). Even so, some noise regions persisted

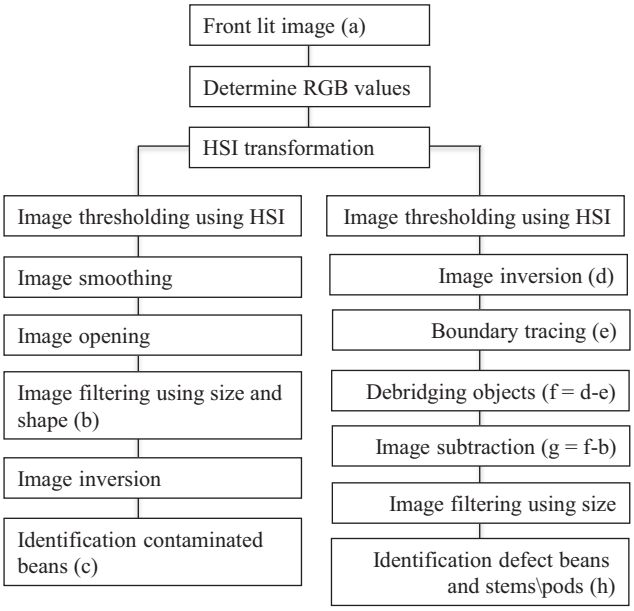

Fig. 8. Flowchart of front lit object identification algorithm.

(Fig. 12(b)) because they were large enough to contain the structuring element. Hence a logical AND operation was applied: first the back lit colour image was split into the constituent RGB channels. Then the B component image was converted to a binary image using a threshold value of 50. The aim of this segmentation step was to identify all target objects (all pixels with intensity value greater than or equal to 50) and remove the background (Fig. 12(c)). The watershed algorithm was applied for boundary tracing of each object (Fig. 12(d)) and then the binary image was subtracted from the boundary tracing image to isolate all touching objects (Fig. 12(e)). Subsequently, size discrimination was applied to remove objects other than beans (Fig. 12(f)). Finally a logical AND operation was used between Fig. 12(b) and (f) to identify only the split beans in the output image. However, small noise regions persisted (pixels from the periphery of normal soybeans) in the output image Fig. 12(g). These noise regions were excluded (Fig. 12(h)) as they were small compared to the projected area (<10,000 pixels) and different in shape (circularity <0.1) compared to the split beans. The final split bean detection algorithm yielded an identification accuracy of 97%.

3.3. Identification results

The algorithms used for front lit and back lit images described above were evaluated using all representative samples tested.

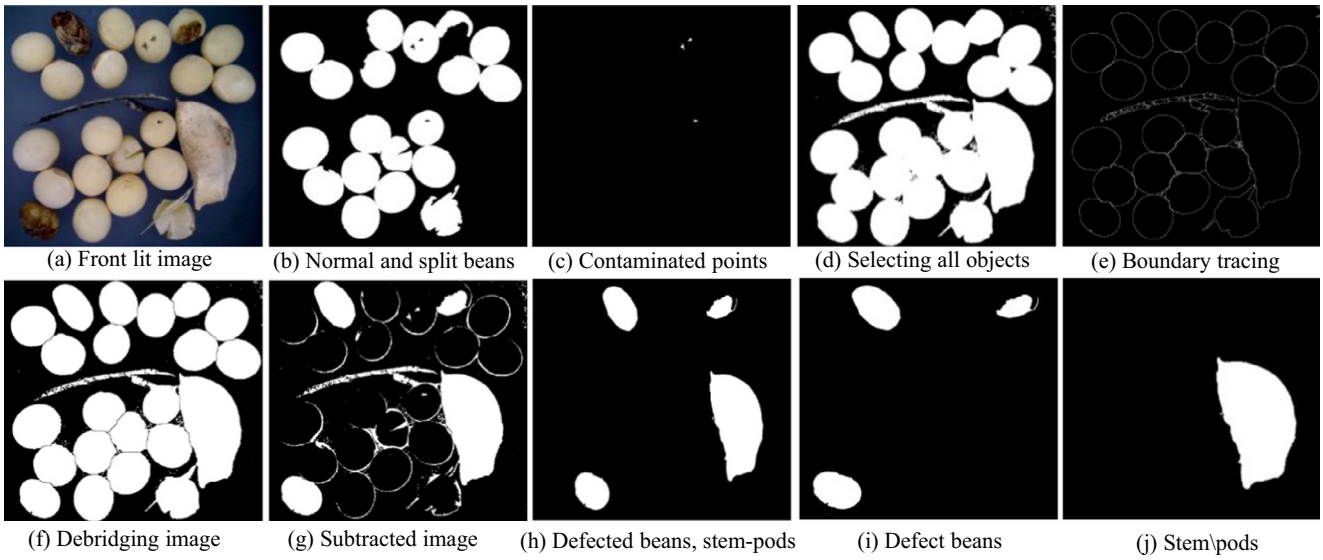

Fig. 9. Front lit image operations performed to detect contaminated beans, defect beans and stem/pods.

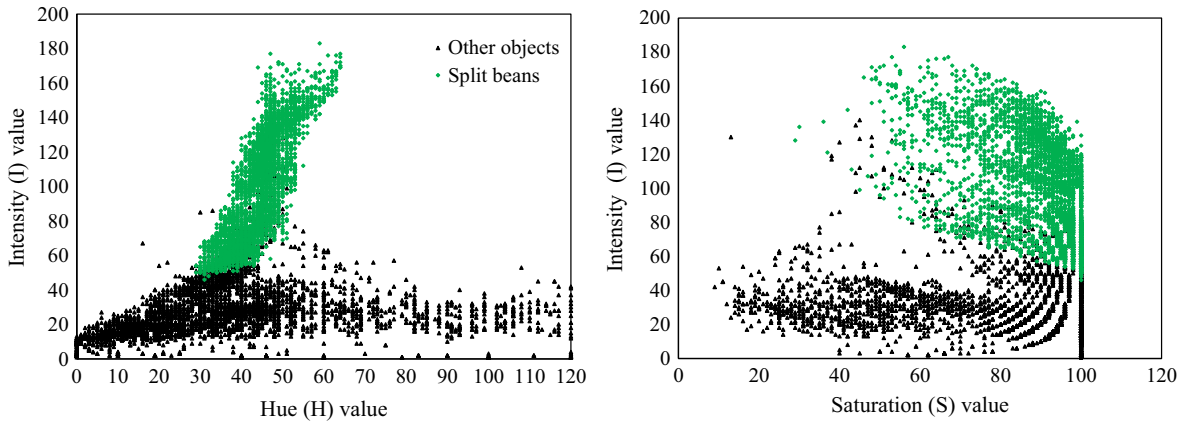

Fig. 10. Back lit image histograms of HSI components of split beans and all other objects.

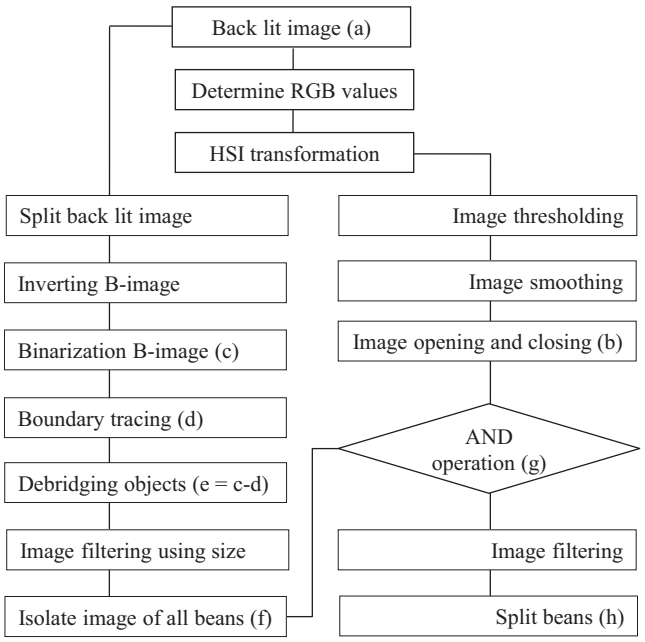

Fig. 11. Flowchart of back lit object identification algorithm.

Table 3 lists the results of detection for various types of object. The resulting image of all processed output images is shown in Fig. 13 (a), in which the green, pink, blue and red colour indicate the normal beans, contaminated beans, split beans, and other objects (defect beans, stems/pods) respectively. It can be readily seen that both the front and back lit image processing algorithms using the HSI colour model served well for identification of the objects.

For the identification of split beans, the detection accuracy using back lit images was 96%. The algorithm was unable to detect highly over threshed cracked beans (3 pieces) shown in Figs. 6 (i) and 13(b). The reason is that the projected area values of these objects were similar those of stem/pods and thus while applying filtering operations those beans were eliminated. The average identification accuracy was 75% for contaminated beans. However, if the contaminated region was located at the periphery of the bean

Table 3
Detection results of various objects present in the harvested grain.

Target objects	Real	Detected	Accuracy (%)
Normal beans	620	620	100
Split beans	70	67	96
Contaminated beans	36	26	75
Other objects	145	143	98

(Fig. 13(c)), it could not be detected since the colour of the contaminated area was similar to the background, yielding a lower identification accuracy for contaminated beans. In addition, sometimes false detection was caused by the umbilicus area of the beans (Fig. 13(d)). The success rate of the algorithm to detect defect beans, and stem/pods was 98%. Finally, the recognition accuracy for normal soybeans was 100%.

3.4. Limitations and future work

The ultimate goal of this project was to develop an efficient, effective, compact and robust machine vision system that is able to provide real time grain quality information to combine operators. The current study represents a first phase, in which the technical feasibility of grain quality monitoring using a front and back lighting based image acquisition system in combination with image processing was evaluated. It was clear beforehand that the machine vision system performance would be inversely proportional to the flow density, and hence, that a sparse, preferably single layer, grain flow must be presented to the camera to limit object occlusion. Therefore, the field of view dimensions of the image acquisition system were chosen as 50 mm × 50 mm, resulting from several trials with varying amounts of materials such as 10 g, 15 g and 20 g. It was confirmed that the sample weighing 10 g provided images (Fig. 5) with less chance of occlusion compared to 15 g and 20 g samples (Fig. 14). Although occlusion may severely reduce detection power, the watershed transform algorithm was able to isolate touching objects for single layer images as described.

The second phase of the project will entail integration of the proof of concept with a harvester. One of the challenges is installation of the system above the grain tank, such that images can be captured of grain flowing through the detection windows. To

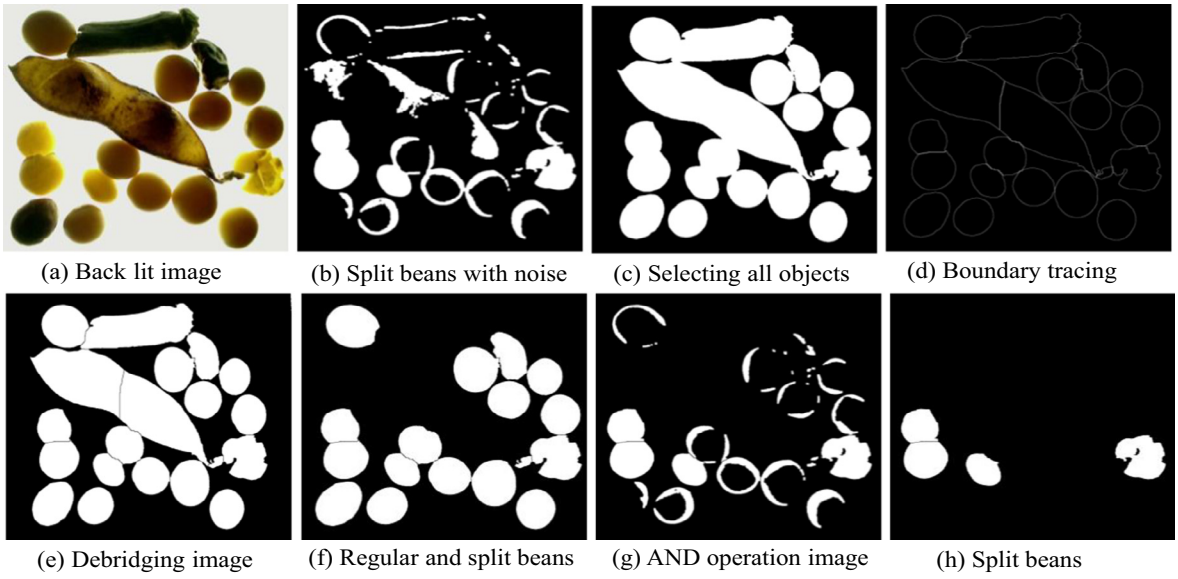

Fig. 12. Back light image processing operations performed for developing split beans detecting algorithm.

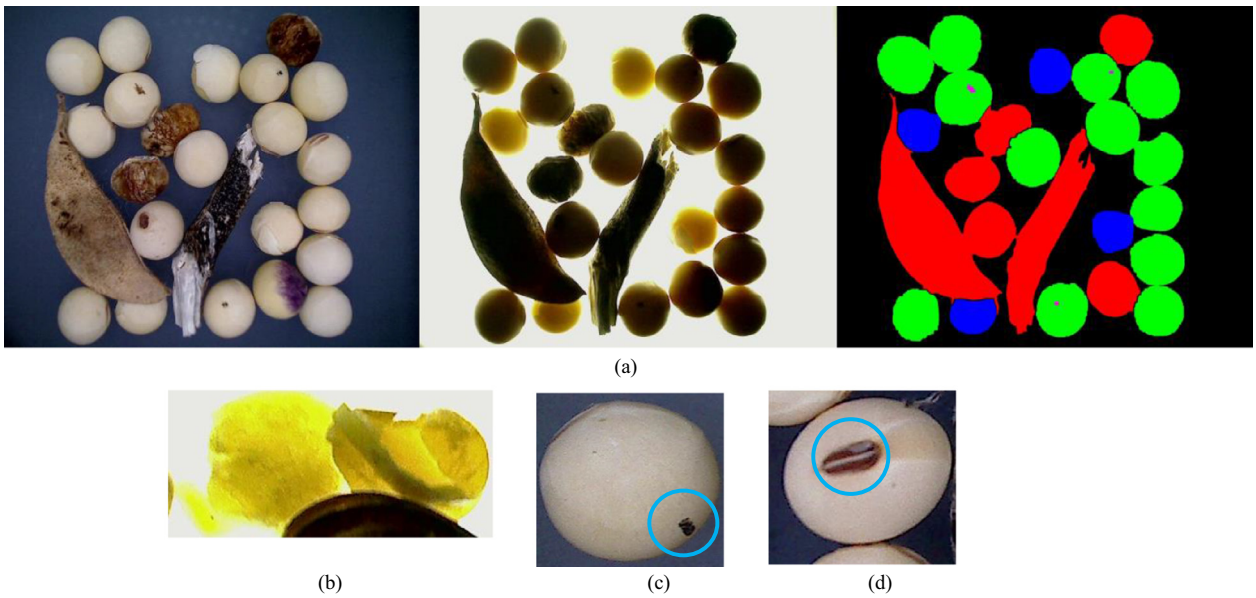

Fig. 13. Example of result image after combining all the front and back lit images (a). Anomalies not detected by the developed algorithm: (b) over threshed split beans, (c) contaminated point located at bean periphery, (d) umbilicus bean.

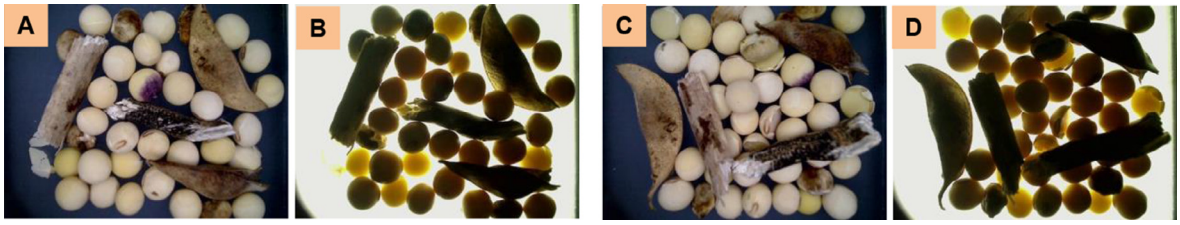

Fig. 14. Example of acquired images of sample weighing 15 g (A. front lit and B. back lit) and 20 g (C. front lit and D. back lit).

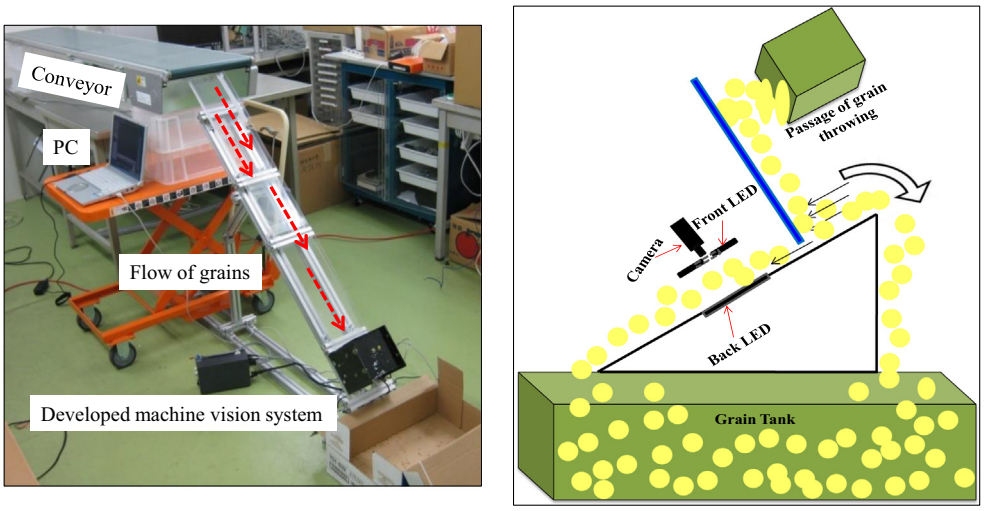

Fig. 15. Experimental setup of the image acquisition system at 45° angle (left). Concept of integrating the MOG detection system at the top of a grain tank (right).

acquire images under dynamic conditions, preliminary experiments were conducted, where the grain flowed at varying downward angles along a flat smooth surface (Fig. 15 (left)). To control the grain flow density along the flow surface, a gate is envisioned, which' opening level can be controlled using the machine vision system itself as the feedback element (Fig. 15 (right)).

4. Conclusions

A proof of concept of a real-time grain quality system to be integrated into a soybean harvester was developed. The aim was to detect common anomalies from clean undamaged soybeans, also known as dockage fractions, allowing targeted adjustment of

combine harvester subsystems to optimize grain quality in the tank. A web camera with back and front lighting was used to evaluate the accuracy of detection of (1) normal (undamaged) beans, (2) split beans, (3) contaminated beans (4) defect beans and (5) stem/pod material. 50 sets of data were collected where a fixed number of these objects were randomly arranged in an imaging cell with a size of 50 × 50 mm. A digital image processing algorithm was able to distinguish each targeted dockage fraction present in the soybean samples based on front lit and back lit images. The developed algorithm successfully identified the target objects with detection rates of 96% for split beans, 75% for contaminated beans, and 98% for defect beans and stem/pods.

Acknowledgements

We acknowledge the financial support and field experiment facilities provided by the Yanmar Co. Ltd. Okayama, Japan.

References

Abdullah, M.Z., Fathinul-Syahir, A.S., Mohd-Azemi, B.M.N., 2005. Automated inspection system for colour and shape grading of star fruit (*Averrhoa carambola* L.) using machine vision sensor. Trans. Inst. Meas. Control. 2 (27), 65–87.

Brosnan, T., Sun, D.W., 2004. Improving quality inspection of food products by computer vision – a review. J. Food Eng. 61 (1), 3–16.

Chen, Y.R., Chao, K., Kim, M.S., 2002. Machine vision technology for agricultural applications. Comput. Electron. Agric. 36, 173–191.

Chetna, V.M., 2013. Machine vision technology for Oryza Sativa L. (rice). Int. J. Adv. Res. Electric. Electron. Instrum. Eng. 2 (7), 2893–2899.

Chun-Liang, C., Din-Chang, T., 2011. Colour image enhancement with exact HSI colour model. Int. J. Innov. Comput. Info. Control. 7 (12), 6691–6710.

Craessaerts, G., Saeys, W., Missotten, B., De Baerdemaeker, J., 2007. A genetic input selection methodology for identification of the cleaning process on a combine harvester, part 2: selection of relevant input variables for identification of material other than grain (MOG) content in the grain bin. Biosyst. Eng. 98 (3), 297–303.

Craessaerts, G., Saeys, W., Missotten, B., De Baerdemaeker, J., 2008. Identification of the cleaning process on combine harvesters. Part 1: a fuzzy model for prediction of the material other than grain (MOG) content in the grain bin. Biosyst. Eng. 101 (1), 42–49.

Gary, B., Kaehler, A., 2008. Learning OpenCV: Computer Vision with the OpenCV Library. O'Reilly, Cambridge, MA, USA.

Gonzalez, R.C., Woods, R.E., 2002. Digital Image Processing. Addison-Wesley, USA.

Gunasekaran, S., 1996. Computer vision technology for food quality assurance. Trends Food Sci. Technol. 7 (8), 245–256. http://dx.doi.org/10.1016/0924-2244(96)10028-5.

Gunasekaran, S., Cooper, T.M., Berlage, A.G., 1988. Evaluating quality factors of corn and soybeans using a computer vision system. Trans. ASAE 31 (4), 1264–1271.

Islas-Rubio, A.R., Higuera-Ciapara, I., 2002. SOYBEAN: Post-harvest operations. Retrieved on March 03, 2016. From <http://www.fao.org/3/a-ax444e.pdf>.

Laungrungthip, N., 2008. Sky Detection in Images for Solar Exposure Prediction. Lincoln University.

Matsui, M., 1999. Threshing unit of head feeding type combine. J. Jpn. Soc. Agric. Mach. 61 (1), 45–46.

Miyamoto, M., Knodo, N., Ogawa, Y., Yamamoto, K., 2015. Combine harvester, Yanmar Co., Ltd, Kyoto University, Japan. Patent No. 5780642.

Novini, A., 1990. Food Processing Automation II. In: Novini, A. (Ed.), Proceedings of the 1990 Conference. St. Joseph, Mich.: ASAE: ASABE.

Olson, E., 2011. Particle shape factors and their use in image analysis – part 1: theory. J. GXP Compliance 3 (15), 85–96.

Paliwal, J., Jayas, D.S., Visen, N.S., White, N.D.G., 2004. Feasibility of a machine-vision-based grain cleaner. Appl. Eng. Agric. 20 (2), 245–248.

Rohit, R.P., Jain, K.R., Chintan, K.M., 2011. Unified approach in food quality evaluation using machine vision. Adv. Comput. Commun. (Part III), 239–248

Sumner, P.E., 2000. Harvesting, drying and storage soybeans. University of Georgia Cooperative Extension Service. Retrieved on June 10, 2016. From <http://caes2.caes.uga.edu/engineering/pubs/documents/harvestsoybean.pdf>.

Takahara, K., Hayashi, S., 1996. Cleaner control system for head-feeding combine harvesters. J. Jpn. Soc. Agric. Mach. 58 (3), 125–126.

Tan, K.Z., Chai, Y.H., Song, W.X., Cao, X.D., 2014. Identification of diseases for soybean seeds by computer vision applying BP neural network. Int. J. Agric. Biol. Eng. 7 (3), 43–50.

Wallays, C., Missotten, B., De Baerdemaeker, J., Saeys, W., 2009. Hyperspectral waveband selection for on-line measurement of grain cleanness. Biosyst. Eng. 1 (104), 1–7.